

Defect-modulated thermal transport behavior of BAs under high pressure

Cite as: Appl. Phys. Lett. **121**, 121902 (2022); <https://doi.org/10.1063/5.0113007>

Submitted: 22 July 2022 • Accepted: 01 September 2022 • Published Online: 19 September 2022

 Yongjian Zhou,  Wen-Pin Hsieh, Chao-Chih Chen, et al.



View Online



Export Citation



CrossMark

ARTICLES YOU MAY BE INTERESTED IN

[Recent progress of solid-state lithium batteries in China](#)

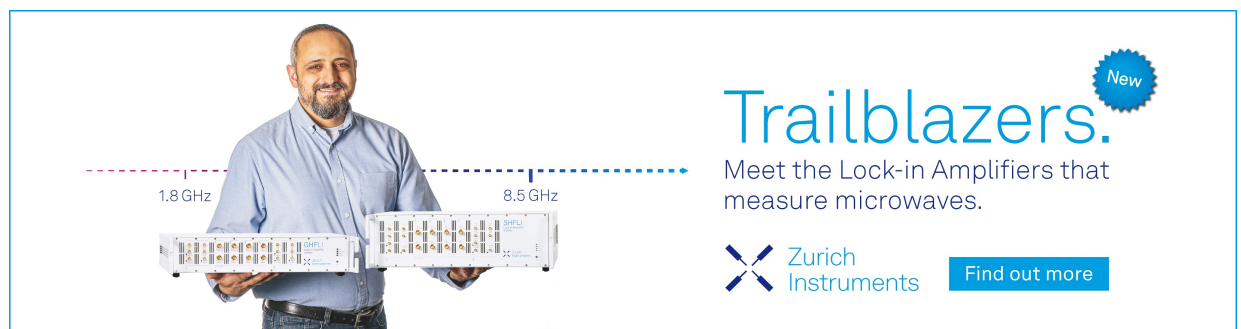
Applied Physics Letters **121**, 120502 (2022); <https://doi.org/10.1063/5.0117248>


[Electrical-field-induced insulator-to-metal transition in samarium monosulfides](#)

Applied Physics Letters **121**, 121901 (2022); <https://doi.org/10.1063/5.0108716>


[Vacancy-induced heterogeneity for regulating thermoelectrics in n-type PbTe](#)

Applied Physics Letters **121**, 122101 (2022); <https://doi.org/10.1063/5.0105597>



Trailblazers. 

Meet the Lock-in Amplifiers that measure microwaves.

 Zurich Instruments [Find out more](#)

Defect-modulated thermal transport behavior of BAs under high pressure

Cite as: Appl. Phys. Lett. **121**, 121902 (2022); doi: [10.1063/5.0113007](https://doi.org/10.1063/5.0113007)

Submitted: 22 July 2022 · Accepted: 1 September 2022 ·

Published Online: 19 September 2022



View Online



Export Citation



CrossMark

Yongjian Zhou,¹ Wen-Pin Hsieh,² Chao-Chih Chen,² Xianghai Meng,¹ Fei Tian,³ Zhifeng Ren,³ Li Shi,^{1,4} Jung-Fu Lin,^{5,a)} and Yaguo Wang^{1,4,a)}

AFFILIATIONS

¹J. Mike Walker Department of Mechanical Engineering, The University of Texas at Austin, 204 E. Dean Keeton Street, Austin, Texas 78712, USA

²Institute of Earth Sciences, Academia Sinica, Nankang, 11529 Taipei, Taiwan

³Department of Physics and Texas Center for Superconductivity at the University of Houston (TcSUH), University of Houston, Houston, Texas 77204, USA

⁴Texas Materials Institute, The University of Texas at Austin, 204 E. Dean Keeton Street, Austin, Texas 78712, USA

⁵Department of Geological Sciences, Jackson School of Geosciences, The University of Texas at Austin, 2305 Speedway Stop C1160, Austin, Texas 78712, USA

^{a)}Authors to whom correspondence should be addressed: afu@jsg.utexas.edu and yaguo.wang@austin.utexas.edu

ABSTRACT

Boron arsenide (BAs) is a covalent semiconductor with a theoretical intrinsic thermal conductivity approaching 1300 W/m K. The existence of defects not only limits the thermal conductivity of BAs significantly but also changes its pressure-dependent thermal transport behavior. Using both picosecond transient thermoreflectance and femtosecond time-domain thermoreflectance techniques, we observed a non-monotonic dependence of thermal conductivity on pressure. This trend is not caused by the pressure-modulated phonon–phonon scattering, which was predicted to only change the thermal conductivity by 10%–20%, but a result of several competing effects, including defect–phonon scattering and modification of structural defects under high pressure. Our findings reveal the complexity of the defect-modulated thermal behavior under pressure.

Published under an exclusive license by AIP Publishing. <https://doi.org/10.1063/5.0113007>

Thermal management posts a critical challenge when power density in electronics keeps scaling up. High thermal conductivity semiconductors that can dissipate heat quickly may help solve this problem as an effective means. As a result, a number of highly thermally conductive materials have been considered for thermal management of high-power electronics.^{1–4} Diamond has the highest thermal conductivity (>2000 W/m K)⁵ but is electrically insulated. Graphite has a high in-plane thermal conductivity close to 2000 W/m K⁶ but with a cross-plane thermal conductivity only less than 10 W/m K,⁷ which limits the heat dissipation capability. Furthermore, the in-plane thermal conductivity of monolayer and few-layer graphene is strongly affected by substrates.⁸ A perfect candidate to help solve this issue would be a bulk semiconductor with high and isotropic thermal conductivity.

Boron arsenide (BAs) is a promising candidate for high-power electronics with thermal conductivity values on the same order of magnitude as those of diamond and graphite along its in-plane direction. As early as 2013, Lindsay *et al.* predicted with *ab initio* calculations that

cubic BAs could have a thermal conductivity as high as 2200 W/m K if only three-phonon scattering is considered.⁹ The large mass ratio between boron and arsenic atoms generates a large energy gap between acoustic phonon and optical phonon branches and greatly suppresses the three-phonon (3-ph) scatterings. This study initiates efforts to grow cubic BAs by a vapor transport technique. In 2018, three independent groups reported high thermal conductivity values measured in cubic BAs, ranging from 900 to 1300 W/m K.^{10–12} Theoretical studies suggested that the discrepancy between the calculation and experiments comes from previously neglected four-phonon (4-ph) scatterings, which was generally ignored in common materials but becomes significant when a large phonon energy gap exists.¹²

Defects present in as-grown BAs affect both the electrical and thermal transports in BAs, hence limiting its applications in electronic devices.¹³ The ultrahigh thermal conductivity values were only observed in certain areas on the as-grown BAs. In general, these as-grown BA crystals possess various types of defects, such as impurity

atoms, vacancies, and dislocations, which can further suppress its thermal conductivity to be lower than 200 W/m K.^{10,14–16} Understanding the fact that how these defects would interact with heat and charge carriers is crucial for designing high-performance electronic devices. Previously, we reported the defect-modulated optical bandgap under high pressure and found that the C and Si defects can form donor-acceptor pairs (DAP) that can trap charge carriers and let them recombine at the defect energy levels.¹⁷ The large compressive strain exerted by a high-pressure environment can also modulate thermal transport behavior via tuning the phonon-phonon scattering, phonon-defect scattering, and even structural defects like dislocations. In this study, we aim to investigate the defect-modulated thermal transport behavior of BA crystals under high pressure. We found that the specific trend of thermal conductivity with pressure is a combined effect from both point-defects and structural defects, with a minimal contribution from the competition between various phonon-phonon scattering channels. Our findings reveal the complexity of the defect-modulated thermal transport behavior under pressure.

The BA single crystals used in this study were grown via the chemical vapor transport (CVT) method. Details of the sample growth can be found in a previous report.¹⁷ The sample was cut by a stainless steel special knife to a size of about $150 \times 75 \mu\text{m}^2$ to be placed inside the diamond anvil cell (DAC) for high-pressure measurements. The DAC device consists of two diamond cutlets of $\sim 400 \mu\text{m}$, and a Re gasket pre-indented to approximately $50 \mu\text{m}$ thick and drilled with a hole of $200 \mu\text{m}$ for the sample chamber. Silicon oil was filled into the chamber as a pressure transmitting medium due to its low thermal conductivity.¹⁸ The pressure is measured *in situ* with the fluorescence of a few ruby spheres placed near the sample, with a typical uncertainty of less than 1 GPa in the pressure range of our study.

The picosecond transient thermoreflectance (ps-TTR) system consists of a picosecond pump laser as the heating source (Coherent Talisker laser with a pulse width of 15 ps, the central wavelength of 1064 nm, and repetition rate of 200 kHz) and a continuous wave (CW) probe laser (Coherent Verdi 532 nm). An 80 nm thick gold layer is deposited onto the sample surface as a thermal transducer. Both the pump and probe beams are collinearly incident on the sample through a Mitutoyo $10\times$ IR long working distance objective lens, with pump and probe spot sizes being 120 and $10 \mu\text{m}$ ($1/e^2$ diameter), respectively. The reflected probe signal is then monitored by a fast Hamamatsu APD detector (Hamamatsu C5658, 1 GHz bandwidth) and recorded by an oscilloscope (TDS 744A, 2 Gbs sampling rate).

In the time-domain thermoreflectance (TDTR) measurements, the output of a Ti:sapphire laser (Spectra-Physics Mai Tai) with a central wavelength of 785 nm is split into pump and probe beams. Here, an ~ 80 nm thick aluminum (Al) layer is deposited on the sample, serving as a thermal transducer. The pump beam, modulated at 8.7 MHz, heats up the Al layer, causing variations in temperature and optical reflectivity. We monitor the temporal evolution of the temperature by detecting the reflected probe beam intensity. Principles of the TDTR were detailed in the literature.^{19,20}

Thermal conductivities of the BA crystals were measured using both TTR and TDTR systems in high-pressure DACs. The samples measured by TTR and TDTR were different (sample No. 1 and sample No. 2, respectively). For each sample, the thermal conductivities on four selected spots were measured. Thermal reflectance spectra from TTR and TDTR measurements at each given pressure were fitted to

derive the thermal conductivity of the sample, which is plotted in Figs. 1 and 2. In the fitting, the density of the sample at high pressure is calculated using the equation of state of BAs reported in the literature by Ravichandran and Broido.^{21,22}

At ambient pressure, the thermal conductivity values were measured with the ps-TTR range from 600 to 900 W/m-K at selected spots on a single piece of the sample. With TDTR, the values range from 100 to 200 W/m-K, again at different spots on a single piece of the sample (not the same sample used for ps-TTR). Two different samples are used for ps-TTR and TDTR measurements. The thermal conductivity values at ambient pressure show that the sample quality varies drastically, and there is significant chemical inhomogeneity in defect concentrations even on the same sample. This phenomenon has been reported previously.^{23–26}

In our previous work,¹⁷ we conducted the time-of-flight secondary-ion mass spectrometry (TOF-SIMS) measurements and confirmed that the most abundant point defects in our BA samples are Si and C. Both Si and C have four valence electrons in the outermost shell ($3s^23p^2$ for Si and $2s^22p^2$ for C) and hence can replace either boron or arsenic sites and serve as both donors (providing extra electrons) and acceptors (receiving electrons or providing extra holes), respectively.

With TTR measurements of sample No. 1, shown in Fig. 1, at all the four selected positions, the derived thermal conductivity shows an obvious increase with pressure up to ~ 15 – 20 GPa. There may be a decreasing trend at higher pressure, but the uncertainties are too large to be ascertained. The red symbols are experimental results when releasing the pressure (in decompression), which follows well with those of increasing pressure. Error bars are plotted for all ps-TTR measurements. Because ps-TTR only measures the amplitude signal, large uncertainty usually shows up for high thermal conductivity materials. On the other hand, the TDTR measurements on a different BA crystal (Fig. 2) show a first increasing and then decreasing trend at all four selected positions. For example, the thermal conductivity at the first spot increases from 150 W/m K at ambient to 600 W/m K at 12 GPa but then decreases to ~ 400 W/m K at 14 GPa. Since TDTR measures both the amplitude and phase information, the overall uncertainty of TDTR measurements is lower, about 10% to 20% over the pressure range we studied. BAs is known to show large variations from sample to sample and large inhomogeneity even in the same sample. The discrepancy of absolute values of thermal conductivity as well as the pressure of saturation (turning) likely comes from the fact that the TTR and TDTR are performed on different samples. Nevertheless, the first increasing and then decreasing trend was observed in seven out of the eight measurements, suggesting that these trends are universal with important physics behind.

Thermal conductivity can be estimated as $k = 1/3c\nu^2\tau$, where c is the heat capacity, ν is the group velocity, and τ is the phonon lifetime. The overall thermal conductivity is a summation of all phonon modes. Compressive strain applied through pressure in a high-pressure diamond anvil cell would shorten the interatomic distance of the BA lattice and increase its interatomic bonding strength. Heat capacity depends on the density. When the interatomic distance decreases under pressure, density and heat capacity increase. Stronger interatomic bonds give higher phonon group velocity. At the same time, stiffer bonding increases the anharmonic scattering among phonons, which decreases the phonon lifetime and hence the thermal

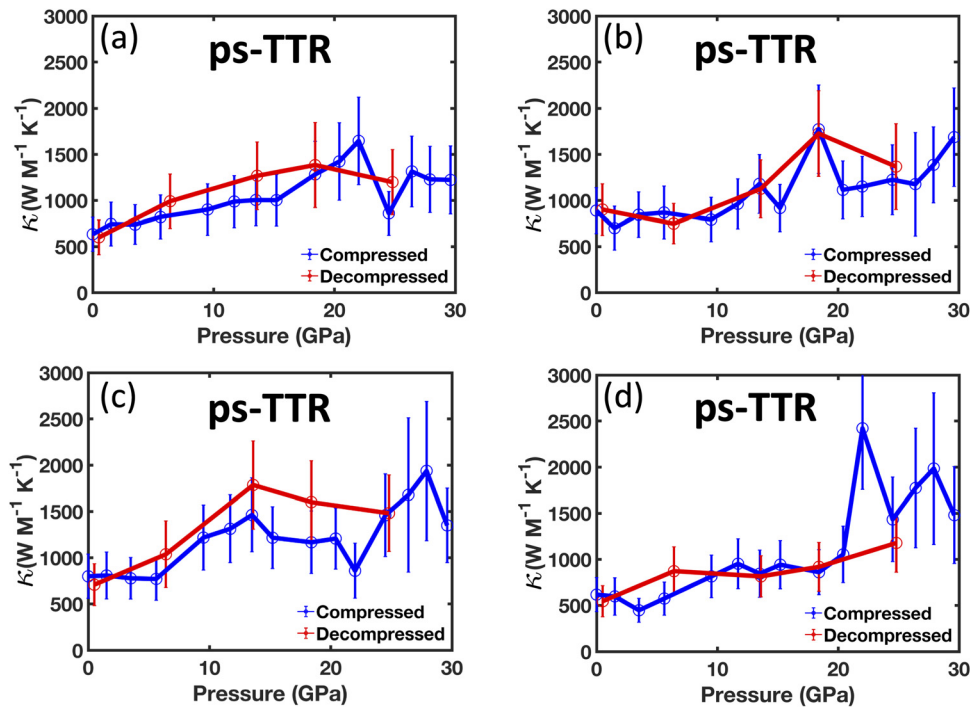


FIG. 1. Pressure-dependent thermal conductivity measured with TTR at selected sample spots on sample No. 1. Both compression (blue open circles) and decompression (red open circles) data were collected from the samples.

conductivity. When the pressure reaches a certain threshold and the interatomic distance is small, it would be more and more difficult to further compress the materials due to the repulsive component of Coulomb interaction among electrons. A combination of these effects could result in the first increasing and then saturation trend with pressure, which has been observed in many covalently bonded solids as well as 2D vdW materials,^{27,28} unless some phase transitions occur. Under this general phenomenon, the first increasing trend observed in BAs is consistent with other materials. What is uncommon is the decreasing trend when the pressure continues to increase.

The first possible reason for this non-monotonic trend (first increasing and then decreasing) could be a phase transition. In some

materials, when the interatomic distance exceeds some threshold, the energy accumulated in the system becomes very high. If there exists another phase that has lower ground energy, the atoms will rearrange according to the new phase. The signature of the emerging new phase is the appearance of new phonon modes. In our previous study, we measured the Raman spectra of BAs up to 20 GPa and observed a fine splitting of LO and TO phonons of isotope ¹¹B. We did not observe any new phonon modes of BAs under high pressure, which indicates that no phase transition occurs in BAs within this pressure range.²⁷

The other factors that need to be considered are the pressure-modulated phonon-phonon interactions, as well as phonon-defect interactions. In BAs, Ravichandran *et al.* predicted an increasing and then decreasing trend of thermal conductivity with pressure, which comes from competing responses of 3-ph and 4-ph scattering processes.²¹ 4-ph scattering has been shown to be important in BAs due to the large energy gap between the acoustic and optical phonon branches, where the 3-ph processes can no longer satisfy the energy conservation and therefore the 4-ph processes are necessary.²¹ The 4-ph scattering rates decrease with pressure, and thus, increase the thermal conductivity, while 3-ph scattering rates increase with pressure and tend to decrease the thermal conductivity. At the low to intermediate pressure region (<20 GPa), the 4-ph reduction effect dominates and gives an overall increasing trend of thermal conductivity with pressure. At the high-pressure region (> 20 GPa), the 3-ph scattering increase dominates and hence the overall thermal conductivity decreases. A peak thermal conductivity appears around 17.5 GPa. Recently, Ravichandran *et al.* also predicted a peak in the pressure-dependent thermal conductivity of boron phosphide (BP) and

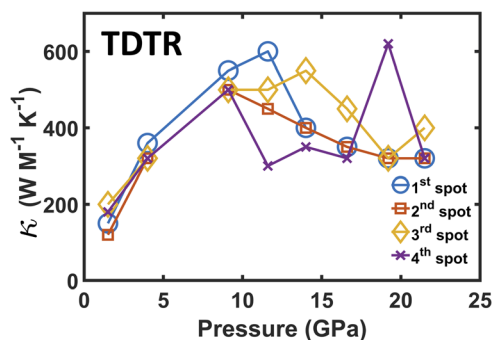


FIG. 2. Pressure-dependent thermal conductivity measured with TDTR at different spots of sample No. 2. The measurement uncertainties are $\approx 10\%$.

attributed it to the interlaying role between 3-acoustic phonon scattering (AAA) and 2-acoustic + 1-optical phonon scattering (AAO).²⁹ For all these calculations, there is only about a 10%–20% increase in thermal conductivity from ambient pressure to the peak. Compared to our experimental results, Fig. 2 shows an increase in about four times in the thermal conductivity, and Fig. 1 shows an increase in about two times. Therefore, the pressure-modulated phonon–phonon interactions are too small to be the dominant mechanism for the observed phenomena in our experiments.

Another key factor to consider would be the phonon–defect interaction. It is well known that the BA samples prepared with current methods suffer from various types of defects that cause inhomogeneity and relatively low thermal conductivity. The two most common types of defects are point defects and structural defects. The point defects would affect the thermal conductivity in two ways: (i) scatter the phonons directly and (ii) provide extra carriers (either electrons or holes) that can also scatter phonons. It is known that boron has two isotopes, ¹⁰B and ¹¹B, whose concentration ratio is about 1:4 in the synthesized BAs. These isotopes would show different behavior under pressure. Our previous study shows that the Raman peak corresponding to ¹⁰B shows a blue shift with pressure, and its intensity drops significantly.¹⁷ The ¹¹B peak split into two peaks at high pressure, corresponding to the splitting of LO and TO phonons. Our previous PL measurements revealed an indirect bandgap around 1.73 eV and two lower transitions corresponding to the donor–acceptor pair (DAP) transitions of Si and C defects (1.4 eV for C-DAP and 1.6 eV to Si-DAP). Under pressure, the indirect bandgap shrinks from 1.73 to 1.62 eV at around 19.2 GPa, and the ionization energy of Si and C donors also decreases by 0.1 and 0.04 eV, respectively. Smaller ionization energy from the defect donor levels means under the same thermal fluctuation background, more carriers initially bound at the defect level could be excited into the conduction band and become free carriers when pressure increases. A first-principles calculation suggested that phonon scattering by a high concentration of free carriers can considerably reduce the lattice thermal conductivity of P-type silicon.³⁰ In comparison, the unique phonon band structure of BA results in not only weak phonon–phonon but also weak electron–phonon scattering, so the effects of free carrier scattering of phonons in the lattice thermal conductivity were not considered as important in recent studies.^{13,31} Furthermore, a recent calculation suggested that ionization of group IV impurities can reduce the bond distortion to decrease impurity

scattering of phonons compared to neutral impurities.³¹ Hence, pressure-induced ionization of impurities can lead to both increased free carrier–phonon scattering and reduced impurity–phonon scattering, resulting in a nontrivial effect on the lattice thermal conductivity.

Structural defects are also abundant in BAs. According to the previous reports, several types of structural defects could exist in the as-grown BA samples, such as micro-cracks,³² twin boundary/grain boundary,¹² and phase segregation.¹³ Under hydrostatic pressure, the compressive strain along all directions would squeeze the microcracks and boundaries, which can increase the thermal conductivity by increasing the interface phonon transmission. At the same time, different phases and grains could shift their locations and orientations, which would also alter the thermal conductivity of the probed area. Hence, the overall effect would depend on a combination of various factors. Figure 3 presents the measurements with TDTR on a sample (sample No. 3) possibly with a large number of structural defects. For the regions initially having low thermal conductivity at low pressure, the values increase with pressure; while for some high-thermal conductivity regions, the values even decrease with pressure. Eventually, the values converge above 30 GPa. These results directly show that applying high pressure reduces the nonuniformity of as-grown BA crystals possibly caused by structural defects. As mentioned before, simulations only predicted about 10%–20% increase in the thermal conductivity in BAs with pressure, so the drastic increase in the thermal conductivity with pressure observed in Figs. 1 and 2 could indicate that some structural defects (such as microcracks and twin/grain boundaries) are compressed to a great extent. At the highest pressures, as shown in Figs. 1, 2, and 3(b), when these defects could not be further compressed, other factors, such as phonon scattering with point defects, would dominate and reduce the thermal conductivity.

We also want to point out some practical difficulties encountered in this study. Ideally, all the experiments should be performed on the same sample and also exactly at the same spot, so a clear correlation between defects and thermal conductivity might be established, which is (unfortunately) not possible at the current stage. It has remained a challenge to grow high-quality BA crystals with low or uniform defect concentration. With either ps-TTR or TDTR measurements, the samples are polished and coated with different thin metal films, making it even more difficult to identify the regions with good quality and perform measurements at same sample/spot between two techniques. For high-pressure measurements, the whole DAC device needs to be taken

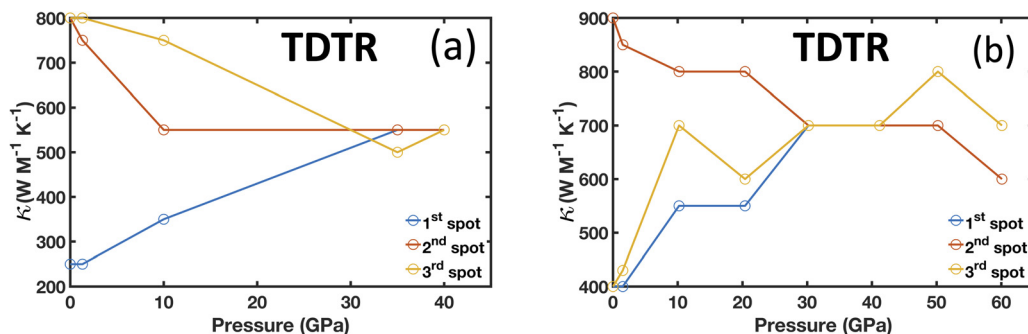


FIG. 3. Pressure-dependent thermal conductivity measured with TDTR at different spots of sample No. 3 with a large number of structural defects. (a) Experiment performed up to 40 GPa. (b) Experiment performed up to 60 GPa. The measurement uncertainties are $\approx 10\%$ before 30 GPa and $\approx 20\%$ at 60 GPa.

out of the spectrometer to adjust the pressure. Even though much care has been taken to measure the same region of the sample, it is impossible to measure on the exact same spot. Furthermore, the samples can be easily damaged under high pressure, so a new sample is used for every set of measurements. Even though with these difficulties, applying both ps-TTR and TDTR does verify the consistency of the observed trend and reveals the rich physics behind.

Finally, we are aware of a recent work posted on arxiv.org about the pressure-dependent thermal conductivity of BAs, which reveals a nearly constant trend with pressure.³³ The discussion of that work focused on the pressure dependence of pure phonon-phonon scattering. As we pointed out earlier, the effect of pure phonon-phonon scattering would only give a change of thermal conductivity of about 10%–20%, comparable with the uncertainty of thermal conductivity measurements, so it is not surprising to observe a constant trend if the phonon-phonon scattering dominates especially in samples without too many defects. According to our discussions above, the thermal conductivity changes measured by both ps-TTR and TDTR show significant changes in the thermal conductivity with pressure, and several physical mechanisms may have contributed to the trend observed in our experiments.

In conclusion, the pressure-dependent behavior of thermal conductivity of as-grown BA samples could exhibit complex features resulting from the competition of different physical mechanisms. Based on the simulation results reported in the literature and our own experimental results, there are five possible mechanisms that can affect the behavior: (i) competition between 3-ph and 4-ph scatterings; (ii) competition between different channels of 3-ph scatterings; (iii) competition between defects-phonon and phonon-phonon scattering; and (iv) pressure could temporarily modify structural defects, which may restore when pressure is released. According to the literature, the first two only consider the intrinsic ph-ph scattering in perfect BA crystals and can induce thermal conductivity change of less than 20%, which is much smaller than what was observed in our experiments. Thus, the behavior observed here should mainly reflect the effects of point defects and structural defects.

The authors are grateful for the support from the National Science Foundation (NASCENT, Grant No. EEC-1160494; Center for Dynamics and Control of Materials DMR-1720595; CBET-2211660); F.T., Z.R., and L.S. were supported by the Office of Naval Research under Multidisciplinary University Research Initiative (Grant No. N00014-16-1-2436).

AUTHOR DECLARATIONS

Conflict of Interest

The authors have no conflicts to disclose.

Author Contributions

Yongjian Zhou: Data curation (equal); Formal analysis (equal); Investigation (equal); Visualization (equal); Writing – original draft (equal); Writing – review & editing (equal). **Wen-Pin Hsieh:** Data curation (equal); Methodology (equal); Writing – review & editing (equal). **Chao-Chih Chen:** Data curation (equal). **Xianghai Meng:** Data curation (equal); Writing – review & editing (equal). **Fei Tian:** Methodology (equal); Resources (equal); Writing – review & editing

(equal). **Zhifeng Ren:** Methodology (equal); Resources (equal); Writing – review & editing (equal). **Li Shi:** Conceptualization (equal); Resources (equal); Writing – review & editing (equal). **Jung-Fu Lin:** Conceptualization (equal); Formal analysis (equal); Resources (equal); Writing – original draft (equal); Writing – review & editing (equal). **Yaguo Wang:** Conceptualization (equal); Formal analysis (equal); Funding acquisition (equal); Methodology (equal); Project administration (equal); Supervision (equal); Writing – original draft (equal); Writing – review & editing (equal).

DATA AVAILABILITY

The data that support the findings of this study are available from the corresponding authors upon reasonable request.

REFERENCES

- X. Qian, J. Zhou, and G. Chen, *Nat. Mater.* **20**(9), 1188 (2021).
- K. Chen, B. Song, N. K. Ravichandran, Q. Zheng, X. Chen, H. Lee, H. Sun, S. Li, G. A. G. Udalamatta Gamage, and F. Tian, *Science* **367**(6477), 555 (2020).
- S. Kumar, M. Nehra, D. Kedia, N. Dilbaghi, K. Tankeshwar, and K.-H. Kim, *Carbon* **143**, 678 (2019).
- V. Guerra, C. Wan, and T. McNally, *Prog. Mater. Sci.* **100**, 170 (2019).
- G. A. Slack, *J. Appl. Phys.* **35**(12), 3460 (1964).
- G. A. Slack, *Phys. Rev.* **127**(3), 694 (1962).
- H. Zhang, X. Chen, Y.-D. Jho, and A. J. Minnich, *Nano Lett.* **16**(3), 1643 (2016).
- J. H. Seol, I. Jo, A. L. Moore, L. Lindsay, Z. H. Aitken, M. T. Pettes, X. Li, Z. Yao, R. Huang, and D. Broido, *Science* **328**(5975), 213 (2010).
- L. Lindsay, D. A. Broido, and T. L. Reinecke, *Phys. Rev. Lett.* **111**(2), 025901 (2013).
- J. S. Kang, M. Li, H. Wu, H. Nguyen, and Y. Hu, *Science* **361**(6402), 575 (2018).
- S. Li, Q. Zheng, Y. Lv, X. Liu, X. Wang, P. Y. Huang, D. G. Cahill, and B. Lv, *Science* **361**(6402), 579 (2018).
- F. Tian, B. Song, X. Chen, N. K. Ravichandran, Y. Lv, K. Chen, S. Sullivan, J. Kim, Y. Zhou, and T.-H. Liu, *Science* **361**(6402), 582 (2018).
- X. Chen, C. Li, Y. Xu, A. Dolocan, G. Seward, A. Van Roekeghem, F. Tian, J. Xing, S. Guo, and N. Ni, *Chem. Mater.* **33**(17), 6974 (2021).
- M. Fava, N. H. Protik, C. Li, N. K. Ravichandran, J. Carrete, A. van Roekeghem, G. K. Madsen, N. Mingo, and D. Broido, *npj Comput. Mater.* **7**(1), 54 (2021).
- Q. Zheng, C. A. Polanco, M.-H. Du, L. R. Lindsay, M. Chi, J. Yan, and B. C. Sales, *Phys. Rev. Lett.* **121**(10), 105901 (2018).
- N. H. Protik, J. Carrete, N. A. Katcho, N. Mingo, and D. Broido, *Phys Rev B* **94**(4), 045207 (2016).
- X. Meng, A. Singh, R. Juneja, Y. Zhang, F. Tian, Z. Ren, A. K. Singh, L. Shi, J. Lin, and Y. Wang, *Adv. Mater.* **32**(45), 2001942 (2020).
- W.-P. Hsieh, *J. Appl. Phys.* **117**(23), 235901 (2015).
- W.-P. Hsieh, B. Chen, J. Li, P. Keblinski, and D. G. Cahill, *Phys. Rev. B* **80**(18), 180302 (2009).
- K. Kang, Y. Kan Koh, C. Chiritescu, X. Zheng, and D. G. Cahill, *Rev. Sci. Instrum.* **79**(11), 114901 (2008).
- N. K. Ravichandran and D. Broido, *Nat. Commun.* **10**(1), 827 (2019).
- F. Datchi, A. Dewaele, Y. Le Godec, and P. Loubeyre, *Phys. Rev. B* **75**(21), 214104 (2007).
- S. Yue, G. A. Gamage, M. Mohebinia, D. Mayerich, V. Talari, Y. Deng, F. Tian, S.-Y. Dai, H. Sun, and V. G. Hadjiev, *Mater. Today Phys.* **13**, 100194 (2020).
- H. Sun, K. Chen, G. A. Gamage, H. Ziyae, F. Wang, Y. Wang, V. G. Hadjiev, F. Tian, G. Chen, and Z. Ren, *Mater. Today Phys.* **11**, 100169 (2019).
- G. A. Gamage, H. Sun, H. Ziyae, F. Tian, and Z. Ren, *Appl. Phys. Lett.* **115**(9), 092103 (2019).
- G. A. Gamage, K. Chen, G. Chen, F. Tian, and Z. Ren, *Mater. Today Phys.* **11**, 100160 (2019).
- X. Meng, T. Pandey, J. Jeong, S. Fu, J. Yang, K. Chen, A. Singh, F. He, X. Xu, and J. Zhou, *Phys. Rev. Lett.* **122**(15), 155901 (2019).

- ²⁸G. T. Hohensee, R. B. Wilson, and D. G. Cahill, *Nat. Commun.* **6**(1), 6578 (2015).
- ²⁹N. K. Ravichandran and D. Broido, *Nat. Commun.* **12**(1), 3473 (2021).
- ³⁰B. Liao, B. Qiu, J. Zhou, S. Huberman, K. Esfarjani, and G. Chen, *Phys. Rev. Lett.* **114**(11), 115901 (2015).
- ³¹J. Shin, G. A. Gamage, Z. Ding, K. Chen, F. Tian, X. Qian, J. Zhou, H. Lee, J. Zhou, and L. Shi, *Science* **377**(6604), 437 (2022).
- ³²F. Tian, B. Song, B. Lv, J. Sun, S. Huyan, Q. Wu, J. Mao, Y. Ni, Z. Ding, and S. Huberman, *Appl. Phys. Lett.* **112**(3), 031903 (2018).
- ³³S. Hou, B. Sun, F. Tian, Q. Cai, S. Wang, W. Peng, X. Chen, Z. Ren, C. Li, and R. Wilson, *arXiv:2110.00215* (2021).